RSC Advances

ROYAL SOCIETY OF CHEMISTRY

www.rsc.org/advances

Journal Name

ARTICLE

Dual energy transfer controlled photoluminescence evolution in Eu and Mn co-activated β-$Ca_{2.7}Sr_{0.3}(PO_4)_2$ phosphors for solid-state lighting†

Received 00th January 20xx,
Accepted 00th January 20xx

DOI: 10.1039/x0xx00000x

www.rsc.org/

Jin Han,‡[a] Fengjuan Pan,‡[b] Wenli Zhou,*[a] Zhongxian Qiu,[a] Miao, Tang,[a] Jing Wang,[b] and Shixun Lian*[a]

Photoluminescence evolution in single-composition phosphors for solid state lighting can be realized through energy transfer strategy, which is commonly based on one sensitizer and one activator. In this work, we focus on a dual energy transfer process, that is, energy transfers from sensitizer Eu^{2+} at two different cation sites to the activator Mn^{2+} at another site in whitlockite-type β-$Ca_{2.7}Sr_{0.3}(PO_4)_2$. Firstly, we refined the crystal structure of the β-$Ca_{2.7}Sr_{0.3}(PO_4)_2$ host by reitveld method. Then we studied the phase, mophorlogy and photoluminescence of Eu and Mn co-activated β-$Ca_{2.7}Sr_{0.3}(PO_4)_2$ phosphors, which are synthesized by conventional solid-state reaction. By adjusting the ratio of Eu^{2+}/Mn^{2+}, the emission hue can be controlled from cyan (0.211, 0.281) to white-light (0.332, 0.290) and eventually to red (0.543, 0.276). The dual energy transfers from Eu^{2+} to Mn^{2+} are demonstrated to be dipole-dipole and quadrupole-quadrupole mechanisms, respectively. Moreover, white light-emitting diodes (LEDs) were fabricated through the integration of 375 nm NUV chip and the white-emitting phosphor $Ca_{2.7}Sr_{0.3}(PO_4)_2$:0.008Eu^{2+}, 0.03Mn^{2+} into a single package, which shows a warm white light with color coordinates of (0.40, 0.41) and correlated color temperature of 3731 K

1. Introduction

White light-emitting diodes (LEDs) are widely used in daily lighting to replace conventional lighting sources. Phosphor-converted (pc-) WLEDs are regarded as a novel lighting source for the next generation.[1-3] As one of the key materials, phosphor play a crucial role in determining the optical quality, lifetime, and cost of pc-WLEDs. Currently, pc-WLEDs are fabricated with the combination of blue InGaN LED chip and yellow-emitting YAG:Ce phosphor.[4, 5] However, the pc-WLEDs based on such combination exhibit poor color rendering index ($Ra < 80$) and high color temperature ($T_c > 7000$ K) due to the lack of red emission.[6, 7] Additionally, it is also possible to produce white light by the combination of tri-color phosphors with ultraviolet (UV) LED chips; while the reabsorption problem commonly causes the poor luminous efficiency.[8, 9] For these reasons, single-composition white emitting phosphors pumped by UV or near-UV chips, which could exhibit excellent Ra values and color stability, have been attracted much attention for solid-state lighting.[10-13]

Generally, white light emitting from a single-composition phosphor is realized through energy transfer strategy. The strategy mainly depends on co-doped systems,[14-17] like Eu^{2+}-Mn^{2+}, Eu^{2+}-Eu^{3+}, Ce^{3+}-Mn^{2+}, and tri-doped systems,[18-23] such as Ce^{3+}/Eu^{2+}-Tb^{3+}-Mn^{2+}. These doping ways just adopt Eu^{2+} or Ce^{3+} with intense absorption to sensitize other luminescent centers and then produce desirable white light emission. As we know, the white light can be formed by the combinations of yellow and blue, or red, green and blue. In co-doping systems, Mn^{2+} or Eu^{3+} centers normally work as the red composition, so the Ce^{3+} or Eu^{2+} needs to emit yellow light for the production of white-light, while the yellow phosphors doped with Ce^{3+} or Eu^{2+} are very rare. In tri-doped systems, Ce^{3+} and Eu^{2+} centers can work as blue composition, Tb^{3+} and Mn^{2+} as green and red one, respectively. It is a good strategy for the production of white-light, but forbidden 4f-4f transition of Tb^{3+} could limit its practical applications due to low luminescence efficiency.[24, 25] Therefore, exploration of new energy transfer way for single-phase white emitting phosphors is desirable.

Rare-earth ions activated phosphate phosphors have been widely studied because of their low sintering temperature, high luminous efficiency and excellent thermal stability. Huang et al. reported the photoluminescence and energy transfer of Ce^{3+}-Mn^{2+} and Ce^{3+}-Mn^{2+} co-activated $Ca_9Y(PO_4)_7$ phosphors for fluorescent lamp application.[13, 26] Li et al. reported tunable blue-green emission in $Ca_3(PO_4)_2$:Eu^{2+}, Tb^{3+} phosphor by energy transfer.[25] Ji et al. reported luminescent and structural

[a] Key Laboratory of Chemical Biology and Traditional Chinese Medicine Research (Ministry of Education of China), Key Laboratory of Sustainable Resources Processing and Advanced Materials of Hunan Province College, College of Chemistry and Chemical Engineering, Hunan Normal University, Changsha, 410081, China.
E-mail: chemwlzhou@hunnu.edu.cn; sxlian@hunnu.edu.cn
[b] School of Chemistry and Chemical Engineering, Sun Yat-sen University, Guangzhou, Guangdong 510275, China.
† Electronic Supplementary Information (ESI) available: The refined crystal structural parameters of β-$Ca_{2.7}Sr_{0.3}(PO_4)_2$ and the lifetimes of Eu^{2+}. See DOI: 10.1039/x0xx00000x
‡These authors contributed equally to this work.

property of yellow-emitting $Sr_{1.75}Ca_{1.25}(PO_4)_2:Eu^{2+}$ phosphor.[27] Recently, they further investigated the cation substitution dependent bimodal photoluminescence in $Ca_{3-x}Sr_x(PO_4)_2:Eu^{2+}$ phosphors.[28] Very recently, we proposed two new strategies, empting site and enlarging sites, to tune the photo-luminescence (PL) of the whitlockite phosphor with multiple cation sites.[29, 30] That work clarified the relation between the sites and PL properties of Eu^{2+}.

Energy transfer from Eu^{2+} to Mn^{2+} has been researched in numerous phosphors. While most of work focus on the energy transfer from one Eu^{2+} site to one Mn^{2+} site, the spectra can only be tuned between one emission band of Eu^{2+} and one of Mn^{2+}. This study intents to enrich the strategies of photoluminescence evolution based on a dual energy transfer. The β-$Ca_{2.7}Sr_{0.3}(PO_4)_2$ compound is selected herein for the following reasons. (1) Eu^{2+} doped β-$Ca_{2.7}Sr_{0.3}(PO_4)_2$ phosphor can present two emission bands, peaking at 417 and 490 nm, respectively. As our previous research, the two bands should be attributed to two different Eu^{2+} luminescent centers, three-fold M(4) sites for the former and eight-coordinated M(3) sites for the latter.[29,30] (2) Photoluminescence evolution based on a dual energy transfer from two Eu^{2+} centers to Mn^{2+} is very rare. (3) Comparison of the dual ET mechanisms in the same phosphor is interesting.

In this work, all the phosphors were successfully synthesized by a high-temperature solid-state technology. The crystal structures, PL evolution, dual energy transfer mechanism, PL thermal stability and performance of WLED package are investigated.

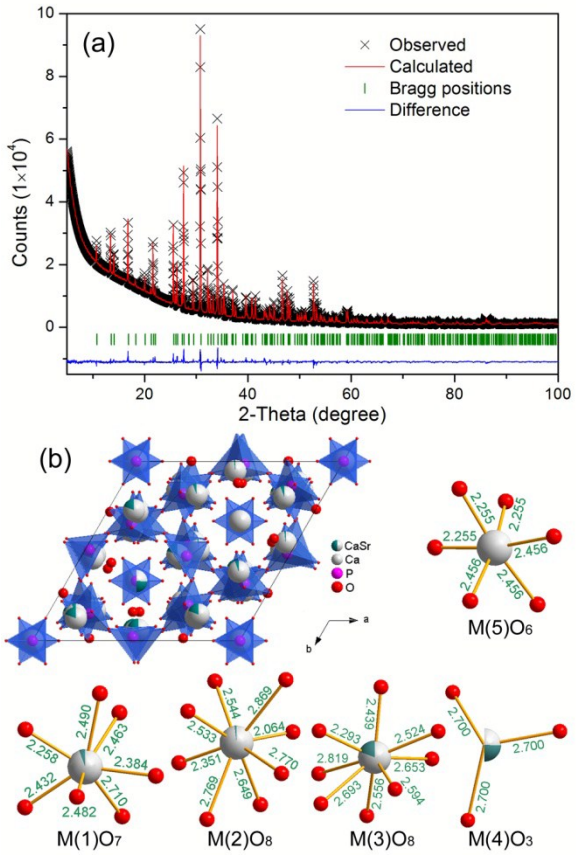

Fig. 1 (a) Rietveld refinements of powder XRD profile of β-$Ca_{2.7}Sr_{0.3}(PO_4)_2$ sample. (b) Schematic structures of the β-$Ca_{2.7}Sr_{0.3}(PO_4)_2$ and Ca/Sr- centered polyhedra.

2. Experimental

2.1 Materials and Synthesis

A series of TCSP:Eu^{2+}, xMn^{2+} (x = 0, 0.03, 0.06, 0.12, 0.24) phosphors were synthesized by conventional solid-state reaction. The concentration of Eu^{2+} in all samples was fixed at 0.008.[31] The starting raw materials, $CaCO_3$ (A. R.), $SrCO_3$ (A. R.), $NH_4H_2PO_4$ (A. R.), $MnCO_3$ (A. R.) and Eu_2O_3 (99.99%), with stoichiometric molar ratios were thoroughly ground and mixed in an agate mortar. The mixtures were preheated at 1000 ^oC for 8 h in air and then sintered at 1100 ^oC for 10 h under a reducing atmosphere of 15% H_2/85% N_2, and slowly cooled to room temperature.

The white-LED package were fabricated by coating a white-emitting phosphor and silicone resin mixture on a NUV LED chip (λ = 375 nm). Air bubbles were removed by vacuum treatment.

2.2 Characterization

The phase purity of all samples was examined by X-ray diffraction (XRD) using a Bruker D8 ADVANCE powder diffractometer with Cu-Kα radiation (λ = 1.54059 Å). High quality XRD data for Rietveld refinement was collected over a 2θ range from 5° to 100° at an interval of 0.02°. The refinement was carried out using the Topas Academic software.[32] The morphology and elemental composition were measured using scanning electron microscopy (SEM, FEI Quanta 400). The photoluminescence excitation (PLE) and photoluminescence spectra in the temperature range 3-500 K as well as fluorescence decay curves were recorded on an Edinburgh FSP920 time-resolved and steady-state fluorescence spectrometer, which is equipped with a time-correlated single-photon counting card and a thermoelectric cooled red sensitive photomultiplier tube. A 450 W Xenon lamp is used as the excitation source. The excitation photons for the fluorescence decay curves are provided by a 150 W nF900 flash lamp. The sample temperature is varied by means of a temperature controller (Oxford, CRY TEMP). The electro-luminescence (EL) spectra were measured using an Ocean Optics QE65000 spectrometer.

3. Results and discussion

3.1 Phase identification and morphology

We first refined the crystal structure of the TCSP compound by the Rietveld method. Fig. 1a shows the observed and calculated X-ray diffraction patterns of TCSP, as well as difference profile of the Rietveld refinement. The crystal data of β-$Ca_3(PO_4)_2$ was used as an initial model for the refinement,[33] which converged to R_{wp} = 3.82% and R_b = 3.48%. The refined crystal structural parameters are shown in Table S1 (ESI). TCSP shows a larger cell volume than β-$Ca_3(PO_4)_2$ due the partial substitution of Sr for Ca. The refined crystal structure of the compound and coordination polyhedra of all

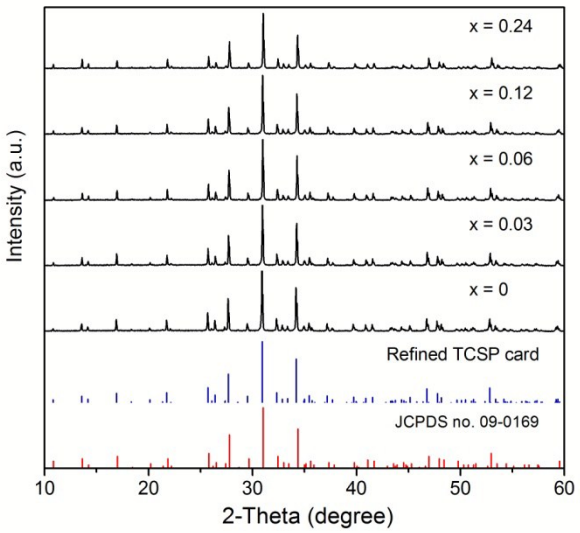

Fig. 2 XRD patterns of $Ca_{2.7-x}Sr_{0.3}(PO_4)_2$:Eu, *x*Mn samples. The refined TCSP card is got from the $Ca_{2.7-x}Sr_{0.3}(PO_4)_2$.cif file by diamond software.

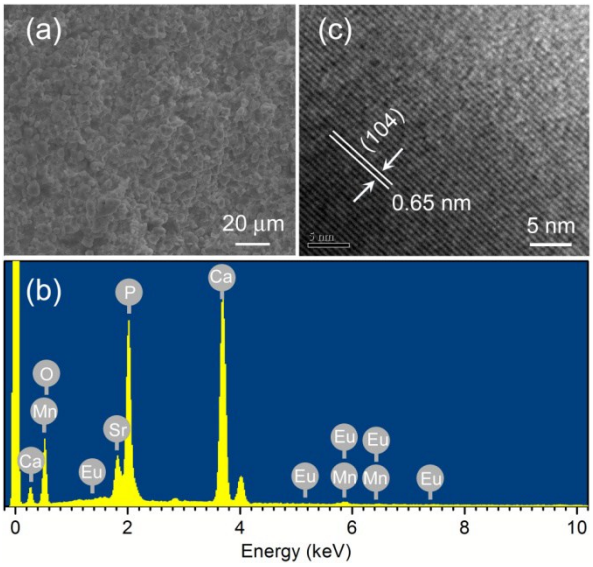

Fig. 3 (a) SEM, (b) EDX and (c) HRTEM images of TCSP:Eu^{2+}, Mn^{2+}.

five M cation sites are sketched in Fig. 1b. The refined occupation fractions of Ca and Sr are 0.9443 and 0.0557 at M(1), 0.9802 and 0.0198 at M(2), 0.8079 and 0.1921 at M(3), 0.2529 and 0.2471 at M(4), 1 and 0 at M(5), respectively. The refinement results reveal that Sr atoms preferentially occupy the 3-fold M(4) sites (Nearly 50% is replaced), then the 8-coordinated M(3) sites (about 20%). The M(5) sites are too small to be occupied by Sr atoms. Both the enlargement of Ca sites and preferential occupation of Sr on Ca(4) sites caused by the substitution of Sr for Ca could result in the migration of some Eu^{2+} activators from M(4) to M(3) sites in TCSP:Eu^{2+}, then one can expect that one emission band (violet-blue) will became two bands (violet-blue and cyan).[29]

The composition and phase purity of all Eu^{2+} and Mn^{2+} co-doped TCSP samples were also checked by XRD. The XRD patterns are shown in Fig. 2. All the diffraction peaks of the samples can be indexed to rhombohedral structure β-

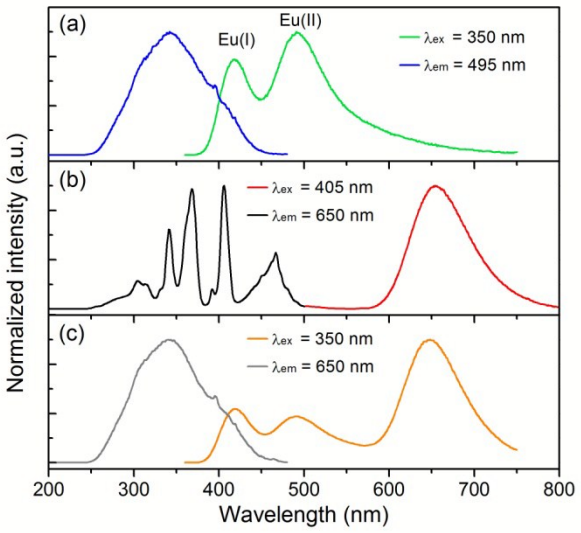

Fig. 4 PLE and PL spectra of (a) $Ca_{2.7}Sr_{0.3}(PO_4)_2$:Eu, (b) $Ca_{2.7}Sr_{0.3}(PO_4)_2$:Mn and (c) $Ca_{2.7}Sr_{0.3}(PO_4)_2$:Eu, Mn samples.

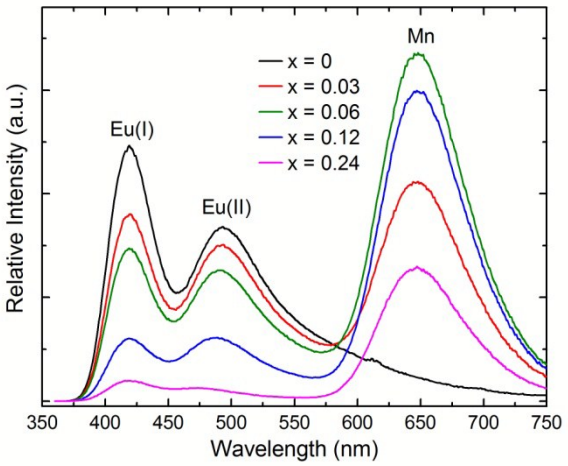

Fig. 5 PL spectra of $Ca_{2.7}Sr_{0.3}(PO_4)_2$:Eu, xMn samples (λ_{ex} = 350 nm).

$Ca_{2.7}Sr_{0.3}(PO_4)_2$ and do not contain any reflections of foreign phases, indicating that the dopants Eu^{2+} and Mn^{2+} are completely dissolved in the TCSP host lattice without inducing significant changes of the crystal structure.

The morphology and elemental composition of TCSP:Eu^{2+}, Mn^{2+} samples were determined using SEM (Fig. 3a). It is found that the particles present smooth morphology and narrow size distribution with diameters of 3-8 micrometers. It is believed that such morphology will be very helpful in the fabrication of white LEDs devices. Energy-dispersive X-ray spectroscopy confirms the existence of the elements Ca, Sr, P, O, Eu and Mn, with atomic ratios of 18.18: 2.16: 14.15: 65.21: 0.16: 0.13. In addition, the well-resolved crystal lattice planes (104) observed from HRTEM image (Fig. 3c) suggest high crystallization of as-prepared phosphors.

3.2 Photoluminescence properties

Fig. 4a-c show the normalized PLE and PL spectra of TCSP:Eu^{2+}, TCSP:Mn^{2+} and TCSP:Eu^{2+}, Mn^{2+} phosphors, respectively. The emission spectrum of TCSP:Eu^{2+} consists of two bands, peaking

at 417 and 490 nm, which are attributed to 5*d*→4*f* transitions of Eu^{2+} occupying the M(4) and M(3) sites of $Ca_{2.7}Sr_{0.3}(PO_4)_2$, respectively.[29] For the two Eu^{2+} centers, here we name them as Eu(I) and Eu(II), respectively. The PLE spectrum (Fig. 4b) of TCSP:Mn^{2+} contains several bands peaked at 304, 341, 368, 405, and 465 nm, corresponding to the transitions from the $^6A_1(^6S)$ level to the $^4T_1(^4P)$, $^4E(^4D)$, $^4T_2(^4D)$, [$^4A_1(^4G)$, $^4E(^4G)$], and $^4T_1(^4G)$ levels of Mn^{2+}, respectively. The PL spectrum centered at 650 nm is assigned to the $^4T_1(^4G) \rightarrow {}^6A_1(^6S)$ transition of Mn^{2+}. The red luminescence is very weak due to the spin- and parity-forbidden *d-d* transition of Mn^{2+}. It is possible to improve the PL of Mn^{2+} through energy transfer from Eu^{2+} to Mn^{2+} due to significant spectral overlap between the emission bands of TCSP:Eu^{2+} and the excitation bands of TCSP:Mn^{2+}. Fig. 4c presents the PLE and PL of Eu^{2+} and Mn^{2+} co-activated phosphor. When monitoring the red emission of Mn^{2+} ions at 650 nm, the excitation spectrum exhibits the extremely similar profiles with that of Eu^{2+} ions, indicating the possibility of energy transfer from Eu^{2+} to Mn^{2+}.

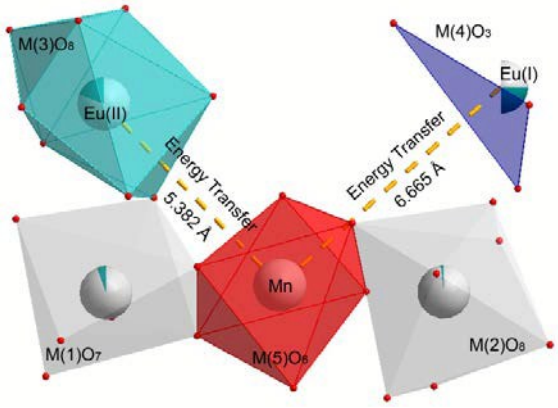

Scheme 1. Dual energy transfer from Eu(I) and Eu(II) to Mn.

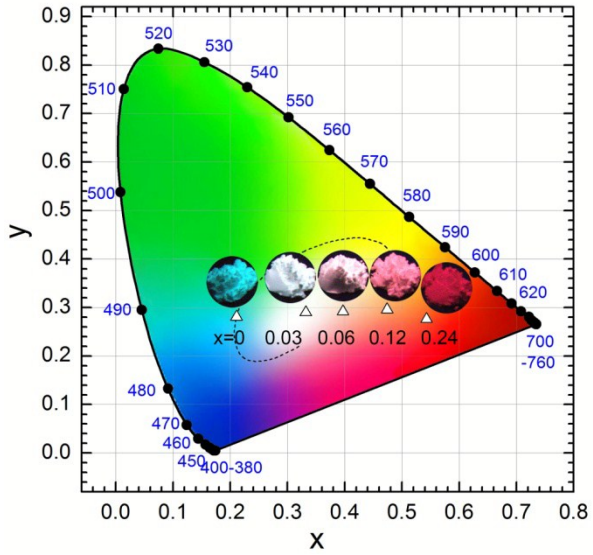

Fig. 6 CIE chromaticity coordination of the TCSP:Eu, *x*Mn phosphors under 350 nm excitation. The insets show luminescence photos of the corresponding phosphors excited under a 365 nm UV lamp.

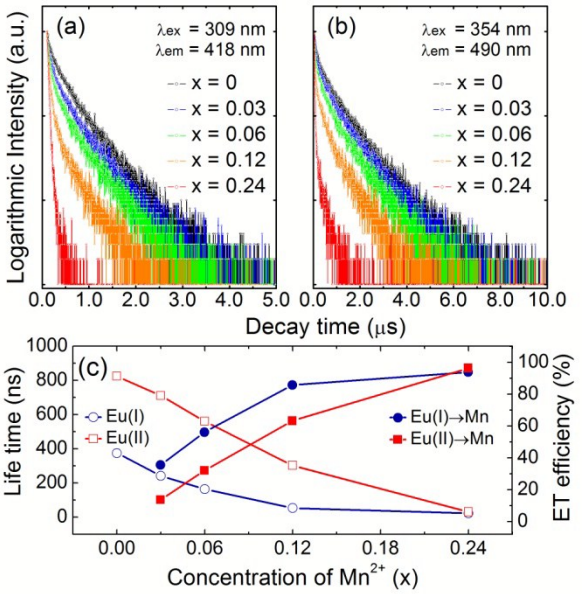

Fig. 7 Decay behavior of $Ca_{2.7-x}Sr_{0.3}(PO_4)_2$:Eu, *x*Mn phosphors. (a) and (b) Decay curves of emission of Eu(I) and Eu(II), respectively. (c) lifetimes of Eu and energy transfer efficiencies of two Eu centers to Mn.

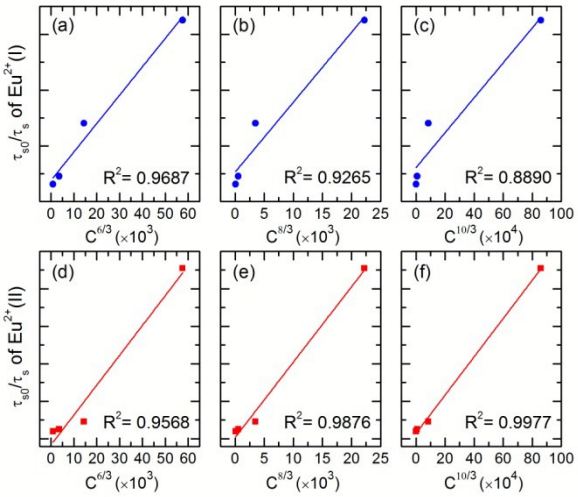

Fig. 8 Dependence of τ_{S0}/τ_S of Eu(I) and Eu(II) on $C^{6/3}$, $C^{8/3}$ and $C^{10/3}$.

Fig. 5 shows emission spectra of TCSP: Eu^{2+}, *x*Mn^{2+} under the excitation at 350 nm. The emission intensity of Eu(I) and Eu(II) decreases with increasing x. In contrast, the emission intensity of Mn^{2+} increases until x = 0.06 and then decreases with further increasing *x* owing to concentration quenching. The observed evolution of PL further supports the existence of dual energy transfer from Eu(I) and Eu(II) to Mn^{2+}. A schematic graph for the dual energy transfer is shown in scheme 1.

The CIE chromaticity diagram of as-synthesized phosphors under 350 nm excitation are shown in Fig. 6. On account of the dual energy transfer from Eu^{2+} to Mn^{2+}, the emission color could be varied from blue-greenish (0.211, 0.281) through white (0.332, 0.290) to red (0.543, 0.276) by tuning the ratio of Eu^{2+}/Mn^{2+}. The CIE color coordinate and calculated correlated color temperature are summarized in Table S3 Above all, we

have obtained white light emission in the single-phase TCSP:0.008Eu^{2+},0.03Mn^{2+} phosphor. The insets of Fig. 6 present the photos of the representative phosphors under irradiation of 365 nm UV-lamp.

3.3 Mechanism of dual energy transfer

The fluorescence decay curves of Eu(I) and Eu(II) as a function of Mn^{2+} concentration (x) are plotted in Fig. 7. The lifetimes can be calculated by fitting with a second-order exponential function according to the following equations[34]:

$$I = A_1\exp(-t/\tau_1) + A_2\exp(-t/\tau_2) \quad (1)$$

$$\tau = (A_1\tau_1^2 + A_2\tau_2^2)/(A_1\tau_1 + A_2\tau_2) \quad (2)$$

where I is the luminescence intensity; τ is the average decay time; A_1 and A_2 are constants; t is the time; and τ_1 and τ_2 are rapid and slow decay lifetimes for exponential components. The values of A_1, τ_1, A_2, and τ_2 are summarized and compared in Table S2 (ESI). The average decay times of Eu(I) are calculated to be 375, 242, 164, 53, and 23 ns, whereas that of Eu(II) are 825, 711, 561, 303, and 30 ns for x = 0, 0.03, 0.06, 0.12, and 0.24, respectively.

Generally, the decay lifetime of the donor center decreases due to the energy transfer from the donor to the acceptor. The efficiency (η_T) of energy transfer from Eu^{2+} to Mn^{2+} can be expressed as[8, 35]:

$$\eta_T = 1 - \tau_S/\tau_{S0} \quad (3)$$

where τ_{S0} and τ_S are the lifetimes of the donor (Eu^{2+}) in the absence and presence of the acceptor (Mn^{2+}), respectively. The lifetimes of Eu^{2+} are found to decrease gradually with increasing doping content of Mn^{2+}. According to the as-calculated lifetimes, the η_T from Eu(I) to Mn^{2+} are estimated to be 35.49%, 56.17%, 85.78%, and 93.85%, and the η_T from Eu(II) to Mn^{2+} are 13.78%, 31.99%, 63.27%, and 96.33% when x is 0.03, 0.06, 0.12, and 0.24, respectively.

The resonant energy transfer mechanisms from sensitizer to activator mainly include exchange interaction and multipolar interaction according to Dexter theory. The critical distance R_C for the energy transfer from Eu^{2+} to Mn^{2+} can be estimated using the concentration quenching method.[35, 36]

$$R_{Eu-Mn} = 2\left[\frac{3V}{4\pi x_C N}\right]^{1/3} \quad (4)$$

where x_C is the critical concentration, N is the number of cation sites in the unit cell, and V is the volume of the unit cell. In our case, N = 21, V = 3562.52 Å^3, and the x_C is the total concentration of the Eu^{2+} and Mn^{2+} ions at which the η_T is 0.5. For the Eu(I) - Mn^{2+} couple, the x_C is 0.088. Accordingly, the R_C of energy transfer from Eu(I) to Mn^{2+} is estimated to be 15.44 Å. In a similar way, the R_C value of Eu(II) - Mn^{2+} is 14 Å. Since the actual concentrations of Eu(I) and Eu(II) are less than 0.008, the actual R_C of energy transfer from Eu(I) and Eu(II) to Mn^{2+} should be larger than the calculated values. Therefore, the R_C values are much longer than 3-4 Å, indicating little possibility of energy transfer via the exchange interaction. Thus, the dual energy transfers from Eu(I) and Eu(II) to Mn^{2+} could take place via an electric multipolar interaction.

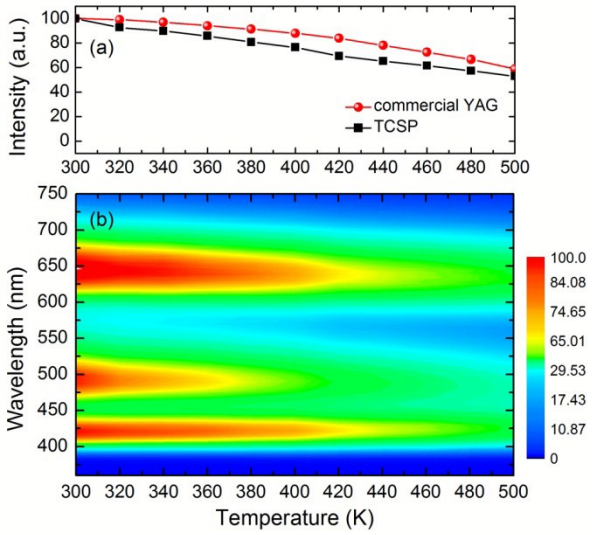

Fig. 9 PL thermal stability of β-$Ca_{2.7}Sr_{0.3}(PO_4)_2$:Eu,Mn phosphor and commercial YAG phosphor.

The energy transfer mechanism can be investigated on the basis of Reisfeld's approximation and Dexter's energy transfer expressions of multipolar interaction[28].

$$\frac{\tau_{S0}}{\tau_S} \propto C^{n/3} \quad (5)$$

where n = 6, 8, and 10 are dipole-dipole, dipole-quadrupole and quadrupole-quadrupole interactions, respectively. C is the doping concentration of the Mn^{2+} ions. The τ_{S0}/τ_S - $C^{n/3}$ plots are further illustrated in Fig. 8a-f, and the relationships can be obtained when n = 6, 8 and 10. The best linear fittings are observed when n = 6 for energy transfer of Eu(I) - Mn^{2+} and n = 10 for Eu(II) - Mn^{2+}, respectively. These results clearly indicate that the energy transfer mechanism from Eu(I) to Mn^{2+} ions is due to a dipole-dipole interaction, whereas that from Eu(II) to Mn^{2+} is a quadrupole-quadrupole interaction.

3.4 Thermal stability

The thermal stability is one of the important technological parameters for phosphor to be used in solid-state lighting, especially in high-power WLEDs.[37] Fig. 9 shows the temperature dependence of PL intensity for TCSP:0.008Eu^{2+}, 0.03%Mn^{2+} phosphor excited at 350 nm. Fig. 9a presents a plot of PL intensity versus temperature. The PL intensity decreases with increasing temperature owing to the thermal quenching. Thermal quenching always occurs due to the non-radiative transition from the excited state of luminescent center to the bottom of conduction band in the lattice.[38, 39] The integrated emission intensity at 100 and 200 °C remains about 80% and 60% in comparison with that at RT. For comparison, the thermal stability of commercial YAG phosphor is also plotted in Fig. 9a (red curve). The results demonstrate that this phosphor has a good thermal stability and might be an excellent candidate for application in pc-WLEDs.

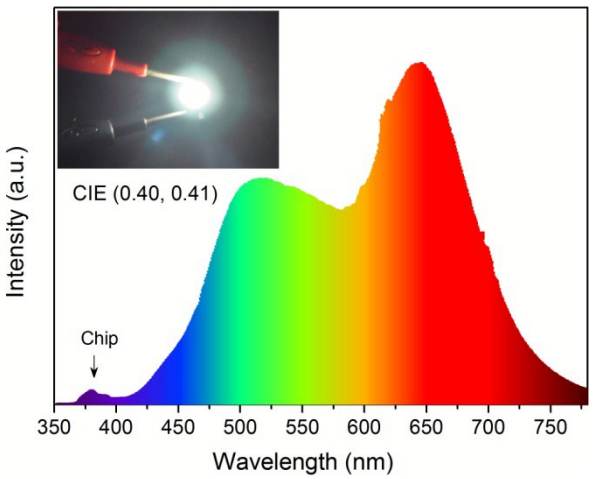

Fig. 10 EL spectrum of a WLED lamp fabricated by coating a white-emitting TCSP:Eu,Mn phosphor on an *n*-UV chip (375 nm) driven by a 350 mA forward bias current. The insets show the photographs of the fabricated WLED lamp and the emission color of the WLED.

3.5 White LED package

Fig. 10 shows the electroluminescence spectrum of the pc-WLED lamp fabricated with the combination of a 375 nm NUV LED chip and a single-phase white-emitting TCSP:0.008Eu^{2+}, 0.03%Mn^{2+} phosphor driven by a 350 mA forward bias current. The electroluminescence spectrum clearly presents three emission bands at 375, 515, and 645 nm, which belong to the NUV LED chip, Eu^{2+} emission, and Mn^{2+} emission, respectively. The optical properties of the pc-WLED lamp give a correlated color temperature of 3731 K and CIE color coordinates of (0.40, 0.41). The inset of Fig. 10 displays the photograph of white light emission from the LED package driven by 350 mA forward bias current. These results indicate that TCSP:0.008Eu^{2+}, 0.03%Mn^{2+} might have promising applications in NUV white-light LEDs.

Conclusions

In summary, a series of single-phase $Ca_{2.7}Sr_{0.3}(PO_4)_2$:Eu^{2+}, Mn^{2+} phosphors have been synthesized by conventional solid-state reaction. The refined crystal structure of $Ca_{2.7}Sr_{0.3}(PO_4)_2$ shows that Sr preferentially occupy the M(4) and M(3) sites, which causes the sensitizer Eu mainly distribute at the two sites. Activator Mn stays at M(5) site. Photoluminescence evolution from blue-greenish to white to red-light could be realize via the dual energy transfer from Eu^{2+} to Mn^{2+}. The mechanisms are proposed to be dipole-dipole and quadrupole-quadrupole interaction for Eu(I)-Mn and Eu(II)-Mn, respectively. Moreover, a pc-WLED lamp combined with 375 nm NUV chip and white-emitting TCSP:0.008Eu^{2+}, 0.03Mn^{2+} phosphor produces a warm white light with color temperature of 3731 K and color coordinates of (0.40, 0.41). These results indicate that TCSP:0.008Eu^{2+}, 0.03Mn^{2+} is a promising single-composition phosphor for application in white-light NUV LEDs.

Acknowledgements

This work is partially supported by the National Natural Science Foundation of China (21501058, 21571059), Hunan Provincial Natural Science Foundation of China (2015JJ2100).

Notes and references

1. M. Shang, C. Li and J. Lin, *Chem. Soc. Rev.*, 2014, **43**, 1372-1386.
2. W.-T. Chen, H.-S. Sheu, R.-S. Liu and J. P. Attfield, *J. Am. Chem. Soc.*, 2012, **134**, 8022-8025.
3. W. B. Im, N. George, J. Kurzman, S. Brinkley, A. Mikhailovsky, J. Hu, B. F. Chmelka, S. P. DenBaars and R. Seshadri, *Adv. Mater.*, 2011, **23**, 2300-2305.
4. M. Shang, J. Fan, H. Lian, Y. Zhang, D. Geng and J. Lin, *Inorg. Chem.*, 2014, **53**, 7748-7755.
5. J. L. Wu, G. Gundiah and A. Cheetham, *Chem. Phys. Lett.*, 2007, **441**, 250-254.
6. A. Aboulaich, M. Michalska, R. Schneider, A. Potdevin, C. Deschamps, R. Deloncle, G. Chadeyron and R. Mahiou, *ACS Appl. Mater. Interfaces*, 2013.
7. H. Zhu, C. C. Lin, W. Luo, S. Shu, Z. Liu, Y. Liu, J. Kong, E. Ma, Y. Cao, R.-S. Liu and X. Chen, *Nat. Commun.*, 2014, **5**.
8. N. Guo, C. Jia, J. Li, Y. Zhao, R. Ouyang and W. Lu, *J. Am. Ceram. Soc.*, 2015, **98**, 1162-1168.
9. A. Kalaji, M. Mikami and A. K. Cheetham, *Chem. Mater.*, 2014, **26**, 3966-3975.
10. Y. Chen, Y. Li, J. Wang, M. Wu and C. Wang, *J. Phys. Chem. C*, 2014, **118**, 12494-12499.
11. Y. Liu, X. Zhang, Z. Hao, X. Wang and J. Zhang, *Chem. Commun.*, 2011, **47**, 10677-10679.
12. C.-H. Huang, P.-J. Wu, J.-F. Lee and T.-M. Chen, *J. Mater. Chem.*, 2011, **21**, 10489-10495.
13. C.-H. Huang, T.-W. Kuo and T.-M. Chen, *ACS Appl. Mater. Interfaces*, 2010, **2**, 1395-1399.
14. Y. Zhang, X. Li, K. Li, H. Lian, M. Shang and J. Lin, *ACS Appl. Mater. Interfaces*, 2015, **7**, 2715-2725.
15. Z. Yang, P.-C. Lin, C.-F. Guo and W.-R. Liu, *Rsc Adv.*, 2015, **5**, 13184-13191.
16. P. Li, Z. Wang, Q. Guo and Z. Yang, *J. Am. Ceram. Soc.*, 2015, **98**, 495-500.
17. W. B. Dai, *J. Mater. Chem. C*, 2014, **2**, 3951-3959.
18. X. Mi, J. Sun, P. Zhou, H. Zhou, D. Song, K. Li, M. Shang and J. Lin, *J. Mater. Chem. C*, 2015, **3**, 4471-4481.
19. S. Deng, Z. Qiu, M. Zhang, W. Zhou, J. Zhang, C. Li, C. Rong, L. Yu and S. Lian, *J. Rare Earths*, 2015, **33**, 463-468.
20. J. Zhang, Y. He, Z. Qiu, W. Zhang, W. Zhou, L. Yu and S. Lian, *Dalton Trans.*, 2014, **43**, 18134-18145.
21. Z. Wang, P. Li, Z. Yang, Q. Guo and G. Dong, *Ceram. Int.*, 2014, **40**, 15283-15292.
22. H. Liu, Y. Luo, Z. Mao, L. Liao and Z. Xia, *J. Mater. Chem. C*, 2014, **2**, 1619-1627.
23. X. Chen, P. Dai, X. Zhang, C. Li, S. Lu, X. Wang, Y. Jia and Y. Liu, *Inorg. Chem.*, 2014, **53**, 3441-3448.
24. M. Xie, D. Li, R. Pan, X. Zhou and G. Zhu, *Rsc Adv.*, 2015, **5**, 22856-22862.
25. K. Li, Y. Zhang, X. Li, M. Shang, H. Lian and J. Lin, *Dalton Trans.*, 2015, **44**, 4683-4692.
26. C.-H. Huang, T.-M. Chen, W.-R. Liu, Y.-C. Chiu, Y.-T. Yeh and S.-M. Jang, *ACS Appl. Mater. Interfaces*, 2010, **2**, 259-264.

27. H. Ji, Z. Huang, Z. Xia, M. S. Molokeev, V. V. Atuchin, M. Fang and S. Huang, *Inorg. Chem.*, 2014.
28. M. Jiao, Y. Jia, W. Lu, W. Lv, Q. Zhao, B. Shao and H. You, *J. Mater. Chem. C*, 2014, **2**, 90-97.
29. J. Han, W. Zhou, Z. Qiu, L. Yu, J. Zhang, Q. Xie, J. Wang and S. Lian, *J. Phys. Chem. C*, 2015, **119**, 16853-16859.
30. J. Han, W. Zhou, M. Tang and S. Lian, *physica status solidi (RRL) – Rapid Research Letters*, 2015, **9**, 485-488.
31. W. Zhou, J. Han, F. Pan, J. Zhang, Q. Xie, S. Lian, L. Yu and J. Wang, *J. Am. Ceram. Soc.*, 2014, **97**, 3631-3635.
32. A. A. Coelho, ed., *TOPAS ACADEMIC*, Brisbane, Australia, 2005.
33. M. Yashima, A. Sakai, T. Kamiyama and A. Hoshikawa, *J. Solid State Chem.*, 2003, **175**, 272-277.
34. S. Lian, Y. Qi, C. Rong, L. Yu, A. Zhu, D. Yin and S. Liu, *J. Phys. Chem. C*, 2010, **114**, 7196-7204.
35. W. Zhou, S. Deng, C. Rong, Q. Xie, S. Lian, J. Zhang, C. Li and L. Yu, *Rsc Adv.*, 2013, **3**, 16781-16787.
36. J. Sun, J. Zeng, Y. Sun and H. Du, *J. Lumin.*, 2013, **138**, 72-76.
37. S. Pimputkar, J. S. Speck, S. P. DenBaars and S. Nakamura, *Nat Photon*, 2009, **3**, 180-182.
38. Z. Xia, J. Zhuang and L. Liao, *Inorg. Chem.*, 2012, **51**, 7202-7209.
39. Z. Xia, R.-S. Liu, K.-W. Huang and V. Drozd, *J. Mater. Chem.*, 2012, **22**, 15183-15189.

Table of contents entry

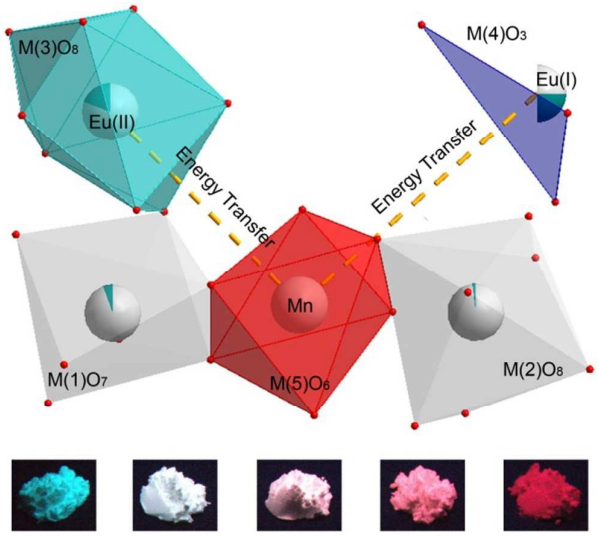

Photoluminescence evolution of a single-composition phosphor for solid state lighting can be realized through a dual energy transfer strategy.